

Supporting Information

A Turn-on Fluorescent Probe for Detection of Sub-ppm level of a Sulfur Mustard Simulant with High Selectivity

Yuanlin Zhang^a, Yanlin Lv^a, Xuefei Wang^a, Aidong Peng^b, Kaiquan Zhang^a, Xiaoke Jie^a, Jijun Huang^{b,*} and Zhiyuan Tian^{a,*}

^aSchool of Chemical Sciences, University of Chinese Academy of Sciences (UCAS), Beijing 100049, P. R. China.

^bCollege of Materials Science and Opto-Electronic Technology, University of Chinese Academy of Sciences (UCAS), Beijing 100049, P. R. China.

*E-mail: zytian@ucas.ac.cn, jjh@ucas.ac.cn

Table of contents

Table S1. Summary of merits of representative fluorescent probes for sulfur mustard (simulant) sensing.

Figure S1. Fluorescence responses of DPXT (10 μ M) to 2-CEES (100 equiv.) recorded at 2 min interval and time-dependent fluorescence responses recorded at 593 nm.

Figure S2. Fluorescence intensity (at 593 nm) enhancement of DPXT in various solvents (10 μ M) upon addition of 100 equiv. of 2-CEES.

Figure S3. (a) Fluorescence emission spectra of DPXT/DCM solution upon gradually increasing the concentration 2-CEES (0-5 μ M). (b) A plot of the fluorescence intensity (at 593 nm) as a function of 2-CEES concentration. The red line is a linear fit to the experimental data ($R^2 = 0.993$).

Figure S4. (a) Photographs of a TLC plate patterned with “CEES” using DPXT/DCM solution acquired before and after exposure to 2-CEES vapor with concentration of 0.5 ppm upon illumination of 365-nm light. (b) Fluorescence emission spectra of the abovementioned TLC plate before (black curve) and after (red curve) exposure to 2-CEES vapor ($\lambda_{\text{ex}} = 570$ nm).

Figure S5. UV-vis absorption (a) and fluorescence emission spectra (b) of DPXT/DCM solution and the DCM solution containing the reference compound xanthene-9-thione (XTT), respectively, in the presence of 100 equiv. of 2-CEES.

Figure S6. Partial ^1H NMR (400 MHz) characterization results of DPXT probe and the thiopyronin product in CD_2Cl_2 .

Figure S7. ^1H NMR characterization result of the DPXT probe (CDCl_3 , 400 MHz)

Figure S8. ^{13}C NMR characterization result of the DPXT probe (CDCl_3 , 100 MHz)

Figure S9. MALDI-MS characterization result of the DPXT probe.

Figure S10. ^1H NMR characterization result of thiopyronin derivative (CDCl_3 , 400 MHz)

Figure S11. ^{13}C NMR characterization result of thiopyronin derivative ($\text{DMSO}-d_6$, 150 MHz)

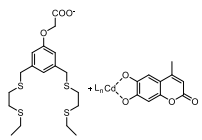
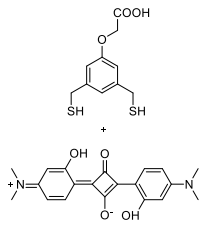
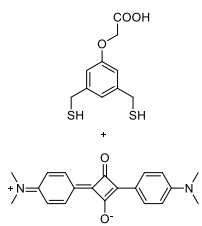
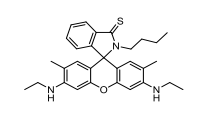
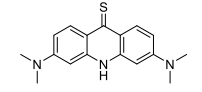
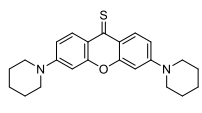
Figure S12. MALDI-MS characterization result of thiopyronin derivative.

Figure S13. ^1H NMR characterization result of XTT (CDCl_3 , 400 MHz)

Figure S14. ^{13}C NMR characterization result of XTT (CDCl_3 , 100 MHz)

Figure S15. MALDI-MS characterization result of XTT

Table S1. Summary of merits of representative fluorescent probes for sulfur mustard (simultant) sensing.

Probe structure	Response time (2-CEES)	Signal enhancement	Limit of detection (LOD)	Test condition	Gas detection	Ref.
	1 min (2-CEES)	~ 4 fold	200 μ M (2-CEES)	80°C, pH=9	No	¹
	1 min (2-CEES)	~ 27 fold	10 μ M (2-CEES)	80°C+K ₂ CO ₃	Yes	²
	1 min (2-CEES)	~ 6 fold	18 μ M (SM)	80°C+K ₂ CO ₃	Yes	³
	>1 h (SM in solution), 10 min (gaseous SM)	~ 100 fold	4.75 μ M (SM in solution), 6.25 ppm /10 min (SM gas)	room temperature	Yes	⁴
	1 min (SM in solution)	~ 25 fold	31.6 μ M (0.005 mg/mL) (SM in solution)	50-60°C , KOH, MeOH	No	⁵
	> 1 h (2-CEES in solution), 2 min (2-CEES vapor)	850 fold (in solution)	1.2 μ M (2-CEES in solution), 0.5 ppm/ min (2-CEES gas)	room temperature	Yes	This work

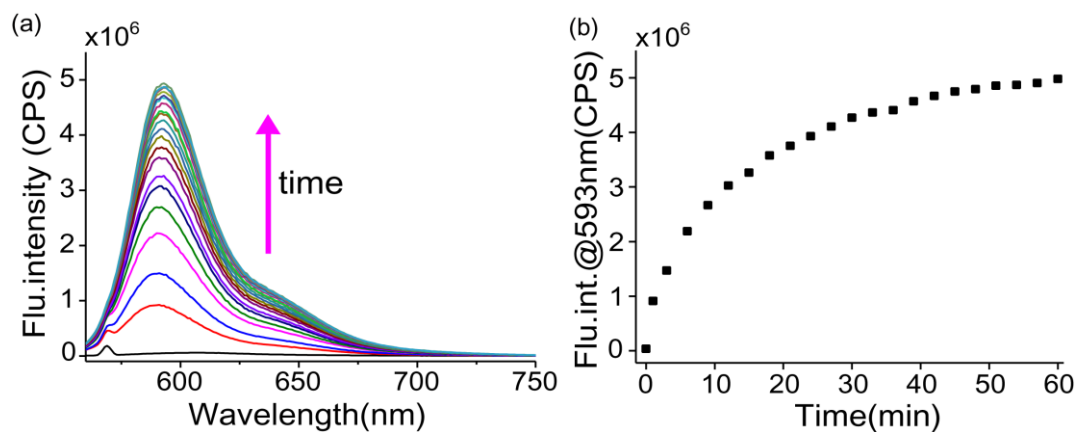


Figure S1. (a) Fluorescence responses of DPXT (10 μ M) to 2-CEES (100 equiv.) recorded at 2 min interval; (b) time-dependent fluorescence responses recorded at 593 nm. $\lambda_{\text{ex}} = 465$ nm

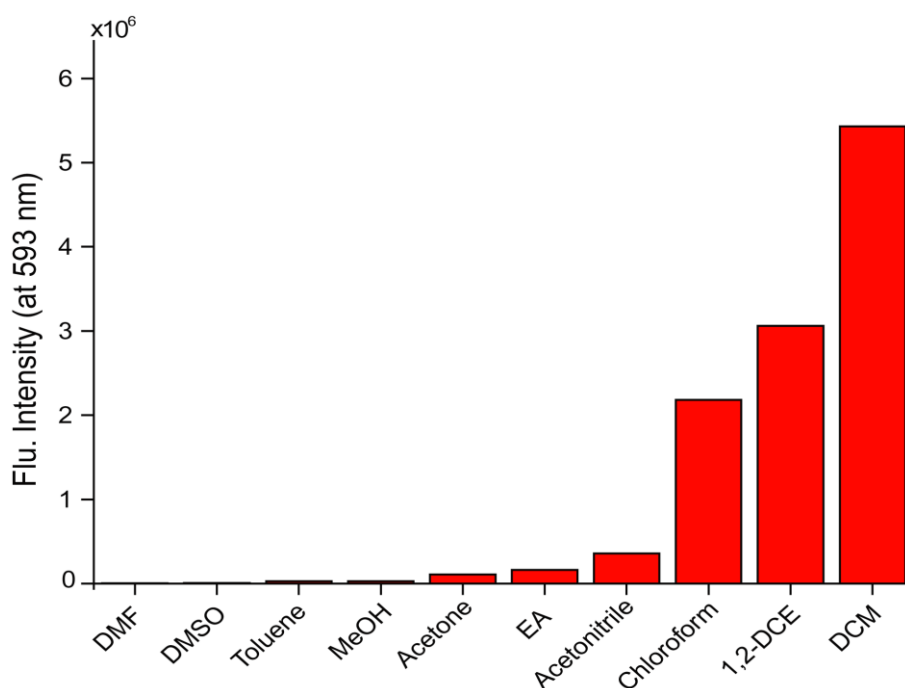


Figure S2. Fluorescence intensity (at 593 nm) enhancement of DPXT in various solvents (10 μ M) upon addition of 100 equiv. of 2-CEES. $\lambda_{\text{ex}} = 570$ nm. Each spectrum was recorded 1 h after the addition of 2-CEES.

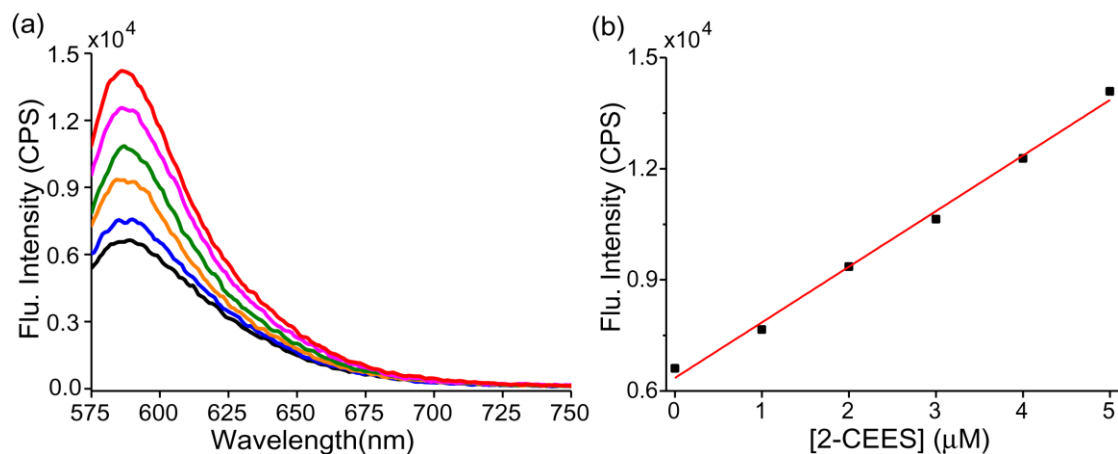


Figure S3. (a) Fluorescence emission spectra of DPXT/DCM solution upon gradually increasing the concentration 2-CEES (0-5 μM). (b) A plot of the fluorescence intensity (at 593 nm) as a function of 2-CEES concentration. The red line is a linear fit to the experimental data ($R^2 = 0.993$).

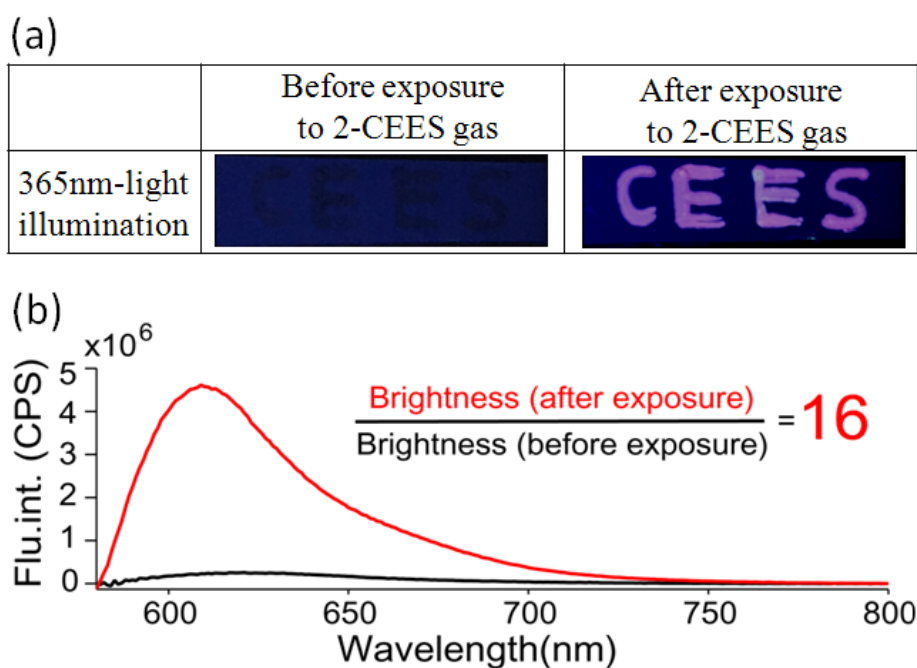


Figure S4. (a) Photographs of a TLC plate patterned with “CEES” using DPXT/DCM solution acquired before and after exposure to 2-CEES vapor with concentration of 0.5 ppm upon illumination of 365-nm light. (b) Fluorescence emission spectra of the abovementioned TLC plate before (black curve) and after (red curve) exposure to 2-CEES vapor ($\lambda_{\text{ex}} = 570 \text{ nm}$).

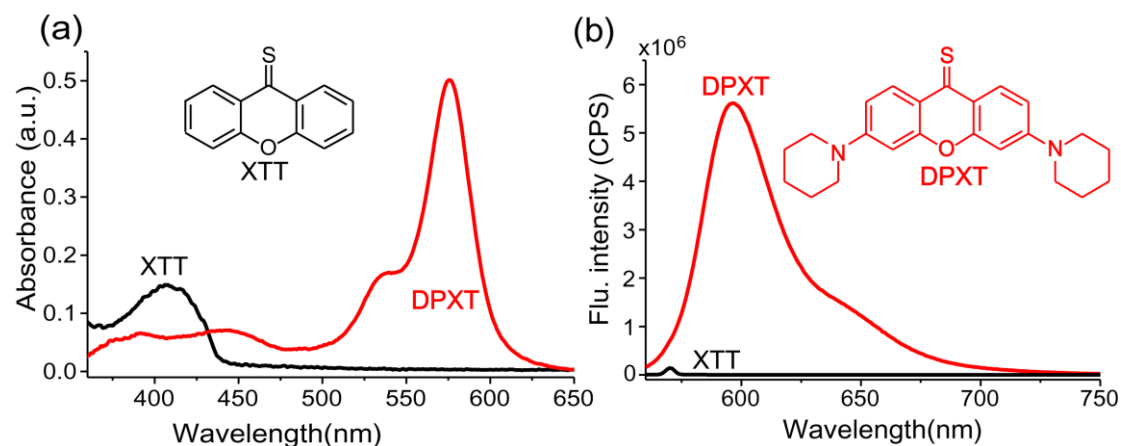


Figure S5. UV-vis absorption (a) and fluorescence emission spectra (b) of DPXT/DCM solution and the DCM solution containing the reference compound xanthene-9-thione (XTT), respectively, in the presence of 100 equiv. of 2-CEES.

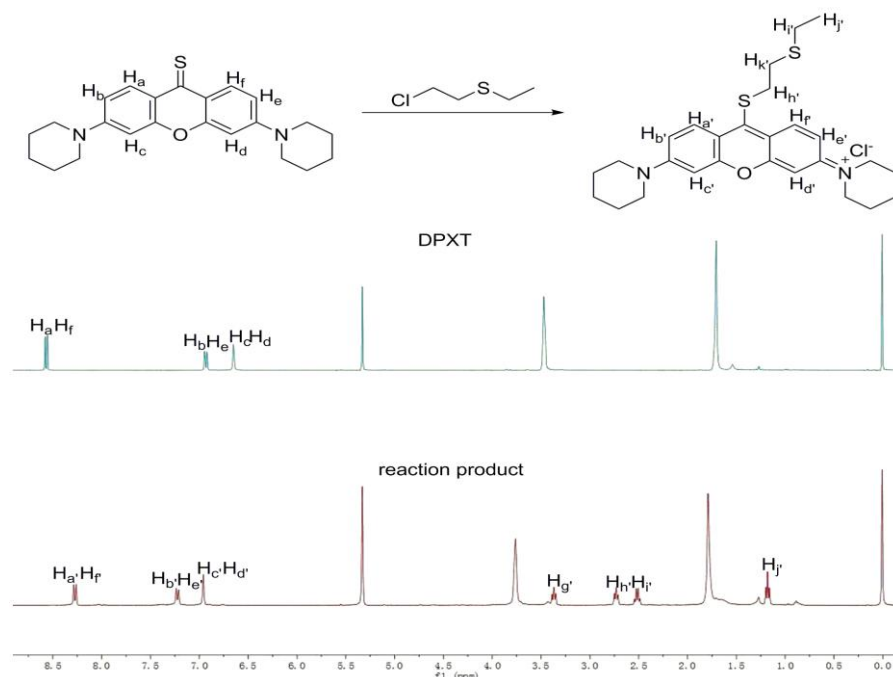


Figure S6. Partial ^1H NMR (400 MHz) characterization results of DPXT probe and the thiopyronin product in CD_2Cl_2

To gain a deeper insight into the underlying mechanism that DPXT underwent, the comparative analysis of the ^1H NMR measurement results of DPXT and the reaction product confirmed the molecular structure of the latter and presented a clue to the underlying mechanism that DPXT underwent. In the presence of CEES, the new signals at 3.37 ($\text{H}_{\text{g}'}$), 2.73($\text{H}_{\text{h}'}$), 2.52($\text{H}_{\text{i}'}$), 1.18($\text{H}_{\text{j}'}$) ppm in the ^1H NMR spectrum

attributable to reaction between DPXT and CEES. Hydrogen signals H_a , H_f (8.55 ppm) shifted to H_a' , H_f' (8.29 ppm) due to the shielding effect, it attribute to the disappearance of the electron-withdrawing thiocarbonyl groups after the reaction of DPXT with CEES. Due to the de-shielding effect of the nitrogen ionization in the piperidyl group, hydrogen signals H_b , H_e (6.95 ppm) and H_b' , H_e' (6.65 ppm) which are adjacent to piperidyl group shift to the low field H_b' , H_e' (7.24 ppm) and H_b'' , H_e'' (6.96 ppm). At the same time, the hydrogen signals in the piperidyl group carbon also moves to the low field significantly. In addition, the proposed mechanism of DPXT probe for 2-CEES sensing also found support from the MALDI-MS characterization results of the DPXT probe sample in the absence and presence of 2-CEES. Specifically, the adduct product of the probe upon addition of 2-CEES displayed characteristic mass-to-charge ratios at 467.2186 (MALDI-MS, $[M]^+$), which is in well agreement with the calculated m/z values of the structures of reaction product. Definitely, the 1H NMR and MALDI-MS characterization results validated the abovementioned proposed sensing mechanism of the as-prepared DPXT probe.

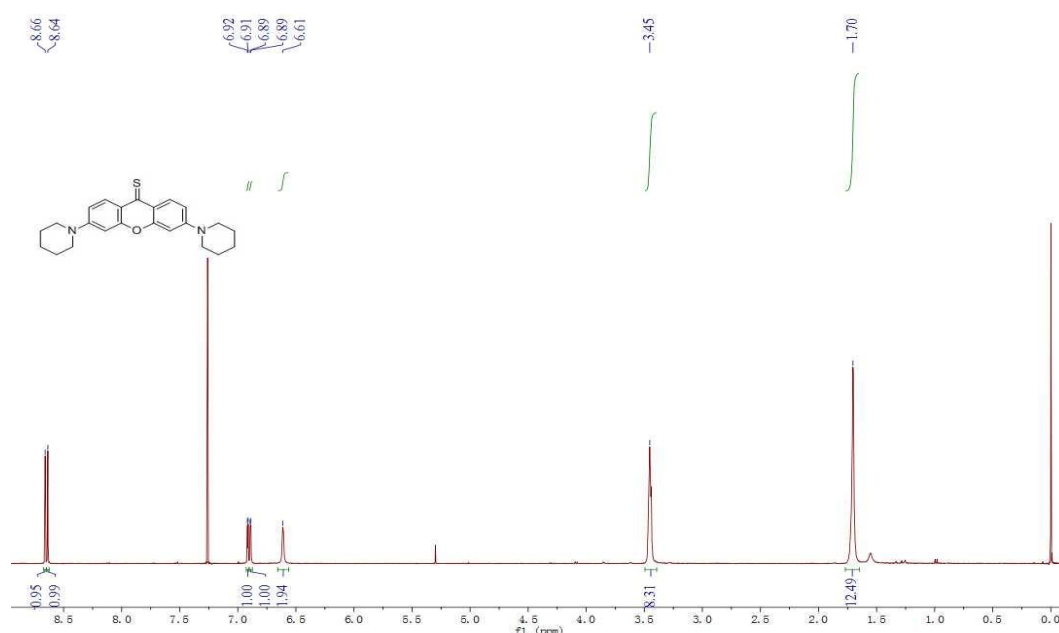


Figure S7. 1H NMR characterization result of the DPXT probe ($CDCl_3$, 400 MHz)

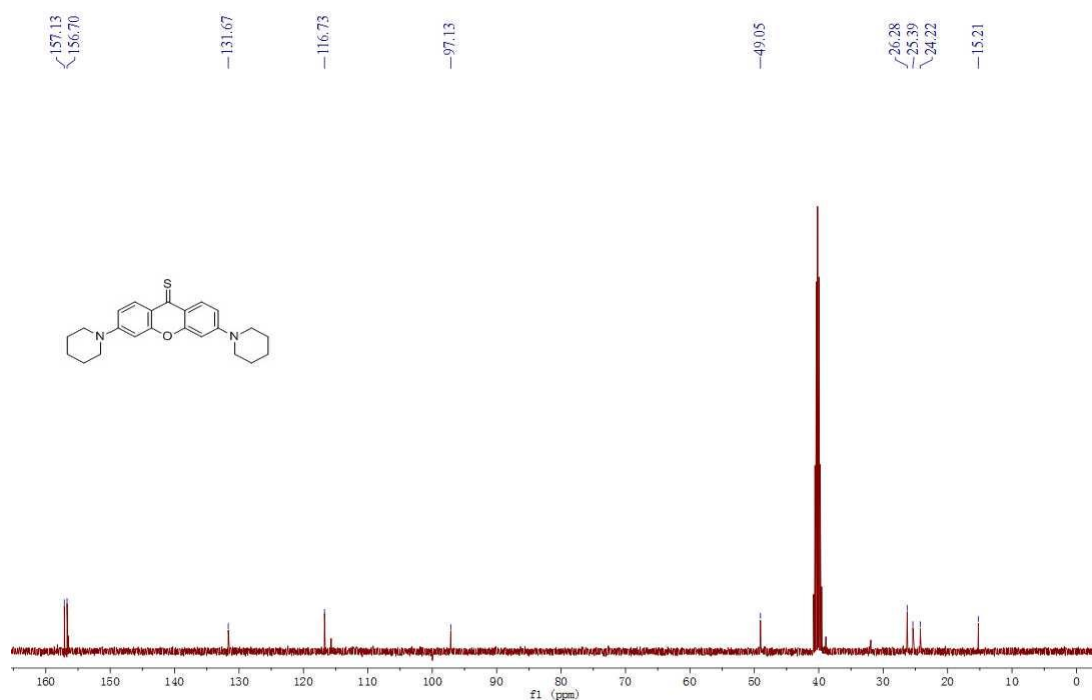


Figure S8. ¹³C NMR characterization result of the DPXT probe (CDCl₃, 100 MHz)

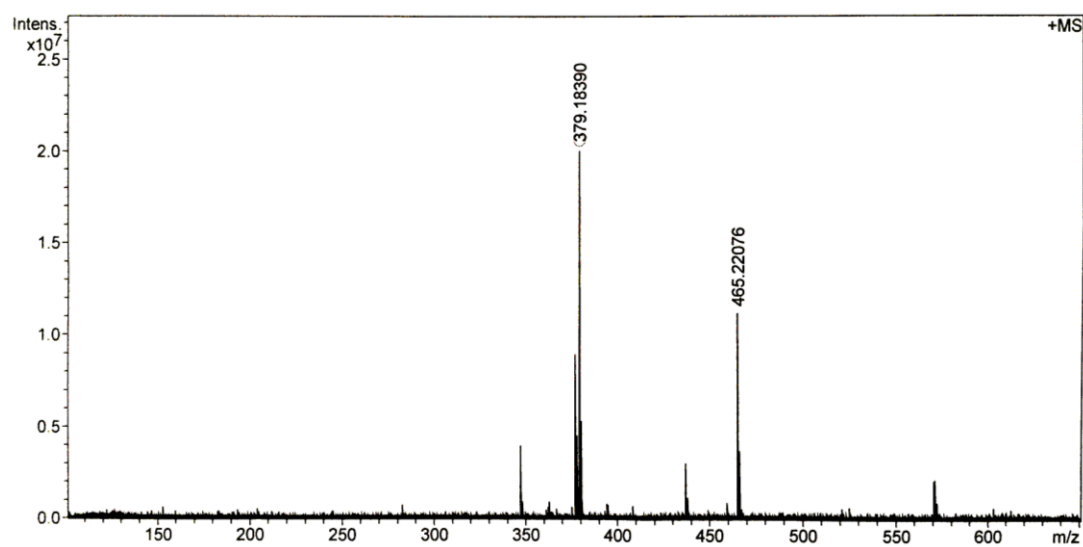


Figure S9. MALDI-MS characterization result of the DPXT probe.

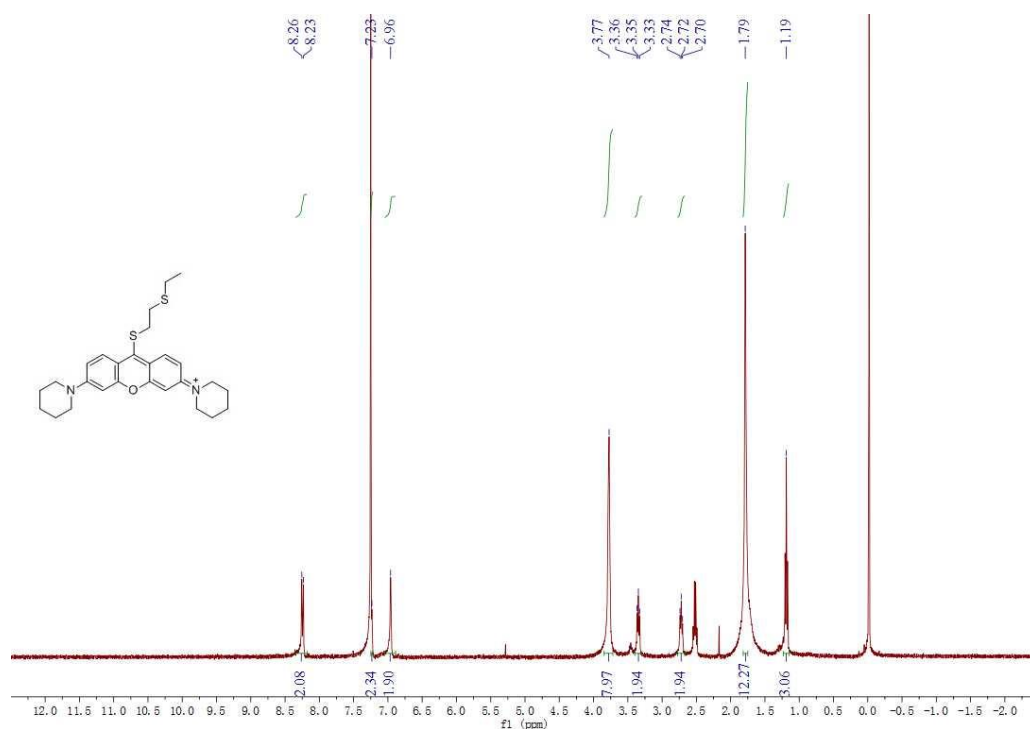


Figure S10. ^1H NMR characterization result of thiopyronin derivative (CDCl_3 , 400 MHz)

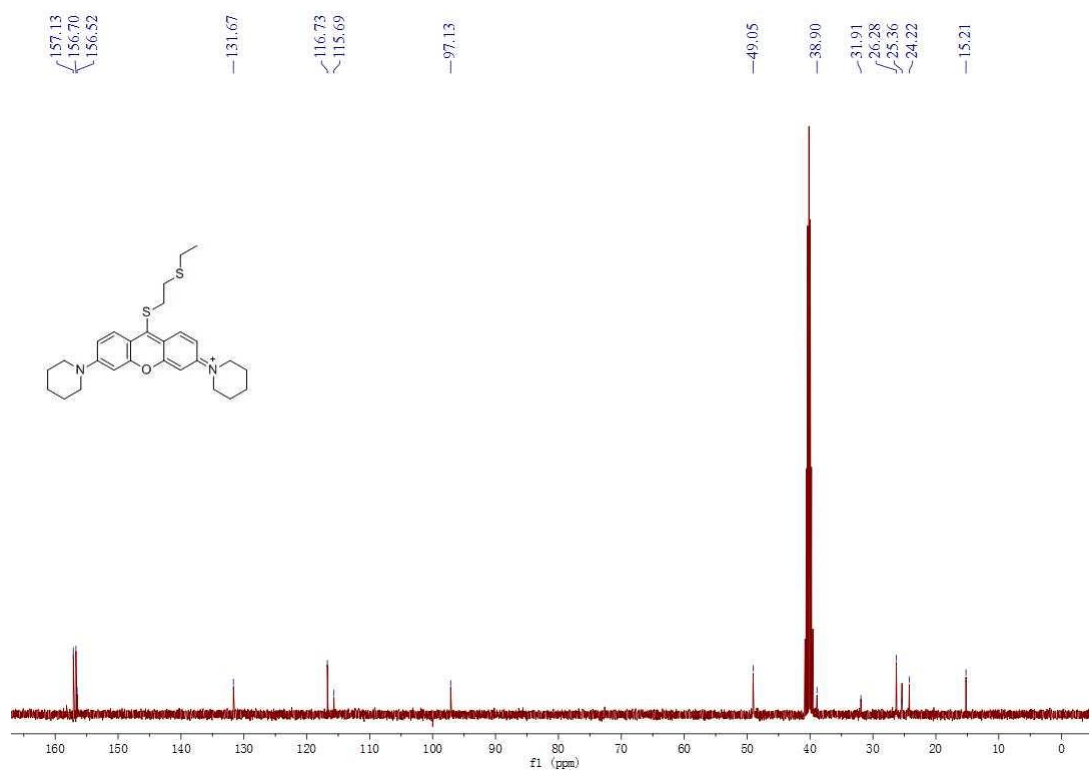


Figure S11. ^{13}C NMR characterization result of thiopyronin derivative ($\text{DMSO}-d_6$, 150 MHz)

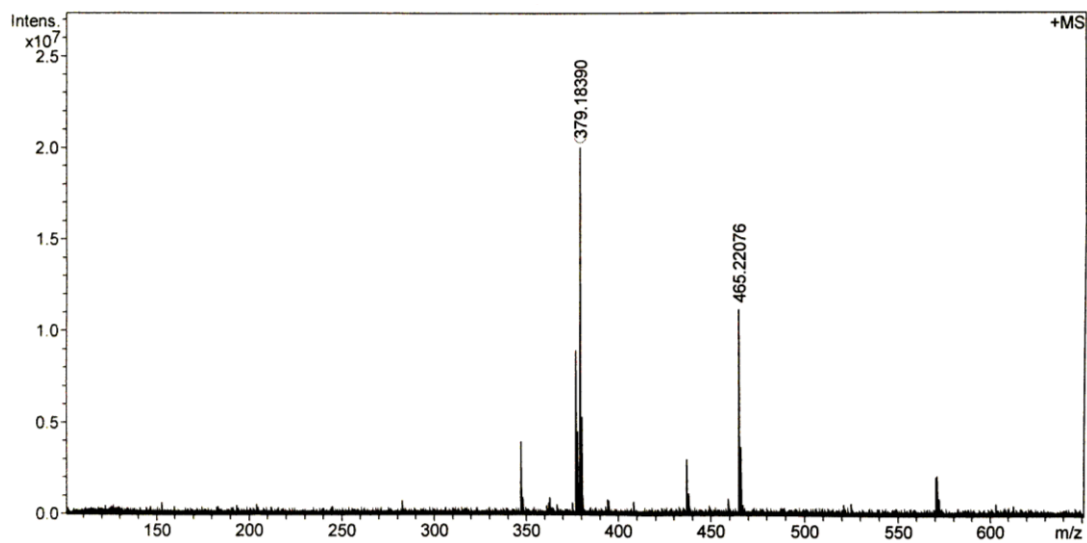


Figure S12. MALDI-MS characterization result of thiopyronin derivative.

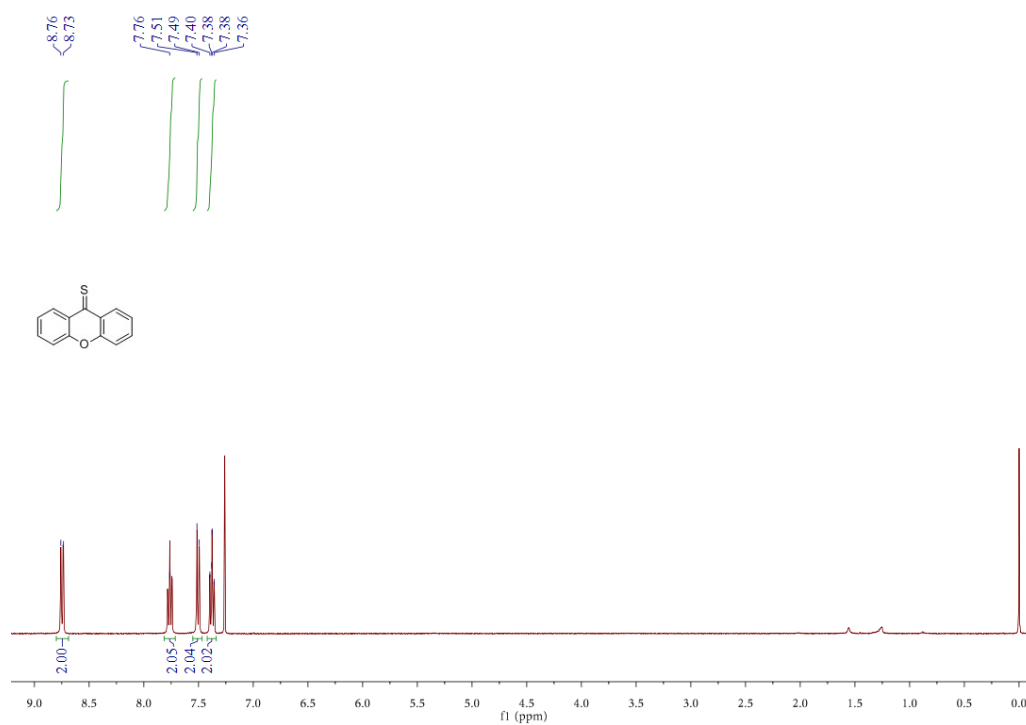


Figure S13. ¹H NMR characterization result of XTT (CDCl₃, 400 MHz).

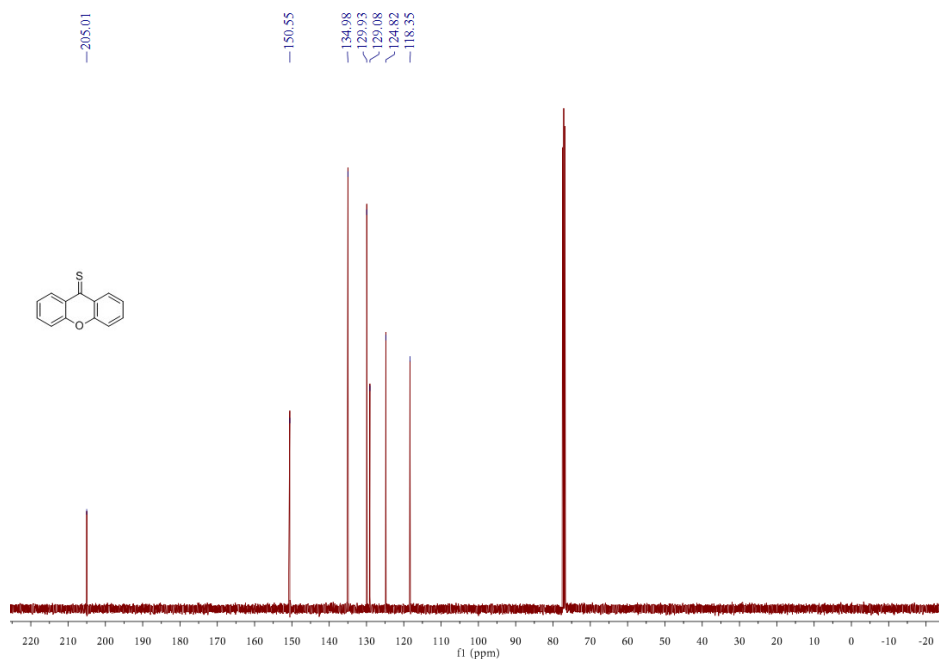


Figure S14. ¹³C NMR characterization result of XTT (CDCl₃, 400 MHz).

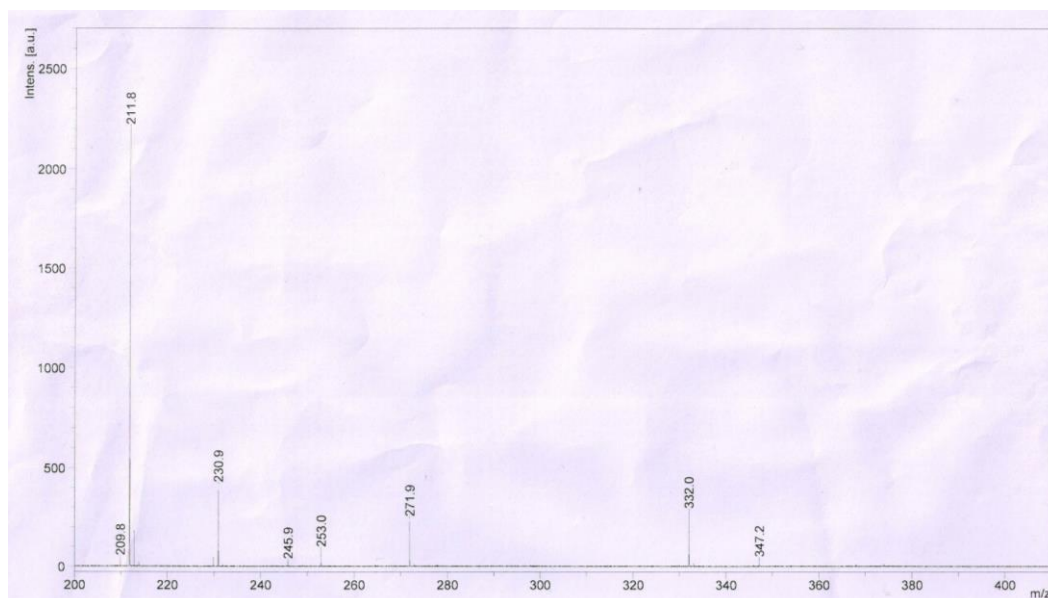


Figure S15. MALDI-MS characterization result of XTT.

References

- (1) Kumar, V.; Anslyn, E. V. *J. Am. Chem. Soc.* **2013**, *135*, 6338-6344.
- (2) Kumar, V.; Anslyn, E. V. *Chem. Sci.* **2013**, *4*, 4292-4297.
- (3) Kumar, V.; Rana, H. *RSC Adv.* **2015**, *5*, 91946-91950.
- (4) Goud, D. R.; Purohit, A. K.; Tak, V.; Dubey, D. K.; Kumar, P.; Pardasani, D. *Chem. Commun.* **2014**, *50*, 12363-12366.
- (5) Kumar, V.; Rana, H.; Raviraju, G.; Gupta, A. K. *Anal. Chem.* **2018**, *90*, 1417-1422.